Achieving Fast and Efficient K⁺ Intercalation on Ultrathin Graphene Electrodes Modified by a Li⁺ Based Solid-Electrolyte Interphase

Jingshu Hui,^{†,¶} Noah B. Schorr,^{†,¶} Srimanta Pakhira,^{‡,§,||,⊥,¶} Zihan Qu,[†] Jose L. Mendoza-Cortes,^{*,§,||,⊥,#} and Joaquín Rodríguez-López^{*,†}

Supporting Information

ABSTRACT: Advancing beyond Li-ion batteries requires translating the beneficial characteristics of Li+ electrodes to attractive, yet incipient, candidates such as those based on K+ intercalation. Here, we use ultrathin few-layer graphene (FLG) electrodes as a model interface to show a dramatic enhancement of K+ intercalation performance through a simple conditioning of the solid-electrolyte interphase (SEI) in a Li⁺ containing electrolyte. Unlike the substantial plating occurring in K+ containing electrolytes, we found that a Li+ based SEI enabled efficient K+ intercalation with discrete staging-type phase transitions observed via cyclic voltammetry at scan rates up to 100 mVs⁻¹ and confirmed as ion-intercalation processes through in situ Raman spectroscopy. The resulting interface yielded fast charge-discharge rates up to ~360C (1C is fully discharge in 1 h) and remarkable long-term cycling stability at 10C for 1000 cycles. This SEI promoted the transport of K+ as verified via mass spectrometric depth profiling. This work introduces a convenient strategy for improving the performance of ion intercalation electrodes toward a practical K-ion battery and FLG electrodes as a powerful analytical platform for evaluating fundamental aspects of ion intercalation.

he technologies beyond Li-ion are gaining momentum by diversifying the energy storage landscape, but strategies are required to improve the performance of electrodes for new types of batteries. Among them, the K-ion battery (KIB) is an emerging candidate compared to Li-ion battery (LIB) due to the reduced cost,1 the availability of high performance cathodes, 2,3 and the more negative anode intercalation potential of K^+ on carbon. 4,5 K^+ storage in various carbon based anode materials has been reported, including graphite,6-9 hard carbon spheres,10,11 highly oriented pyrolytic graphite, 12 graphene foam, 13,14 and reduced graphene oxide.6 Despite the variety, many of these carbon materials exhibit limited cycling stability, in part due to K plating 7,10,14,15 The few reports that demonstrate clear evidence of a staging type intercalation behavior, show sluggish kinetics.^{8,9} Therefore, to improve the performance of KIB anodes, it is necessary to better understand K+ intercalation and to develop straightforward strategies for improving their interfacial properties.

During the early stages of LIB cycling, a layer of decomposition products of solvent and electrolyte known as the solid-electrolyte interphase (SEI) forms on the anode surface. 16,17 While this SEI layer is electronically passivating, preventing further solvent decomposition and Li plating, it remains ionically conductive, allowing for fast Li+ mobility. 18 Therefore, this interfacial layer is crucial for stable intercalation in LIBs. As a comparison, pure K+ containing electrolyte leads to incomplete SEI coverage on KIB anodes,7 and the use of K+ additives in LIB anodes suppresses SEI growth. 19 Poor SEI formation allows K metal plating on the electrode, leading to low cycling rates, capacity losses due to electrode exfoliation, and low cycling efficiency.5 To solve this problem, a highperformance K⁺ conductive SEI layer is required. In this study, we turn to ultrathin nanostructured electrodes of few-layer graphene (FLG)²⁰ as model interfaces to elucidate and expand the possibilities of K⁺ intercalation. We show that a preconditioned SEI layer in Li⁺ containing electrolytes creates a beneficial environment for stable, reversible, and fast K⁺ intercalation in FLG with dramatic improvements in rate and cyclability.

The FLG samples we used were grown using atmospheric pressure CVD and wet-transferred to SiO₂ chips to yield large-area electrodes. ^{21–23} As shown in Figure 1a, the sample

Received: August 27, 2018 Published: October 9, 2018



Department of Chemistry, University of Illinois at Urbana—Champaign, 600 South Mathews Avenue, Urbana, Illinois 61801,

[‡]Discipline of Metallurgy Engineering and Materials Science, Indian Institute of Technology Indore, Simrol, Indore-453552, Madhya Pradesh, India

SDepartment of Chemical & Biomedical Engineering, Florida A&M—Florida State University, Joint College of Engineering, 2525 Pottsdamer Street, Tallahassee, Florida 32310, United States

Department of Scientific Computing, Materials Science and Engineering, High Performance Materials Institute, Florida State University, Tallahassee, Florida 32310, United States

 $^{^\}perp$ Condensed Matter Theory, National High Magnetic Field Laboratory (NHMFL), Florida State University, 1800 E. Paul Dirac Drive, Tallahassee, Florida 32310, United States

Department of Physics, Florida State University, Tallahassee, Florida 32306, United States

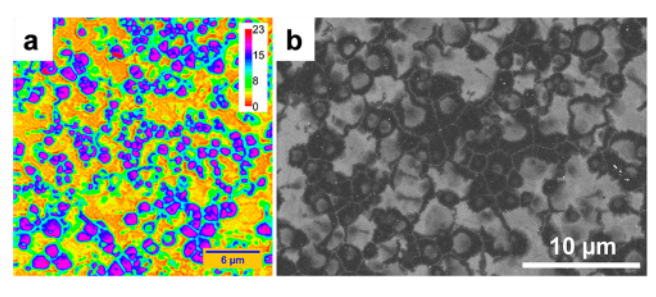


Figure 1. Characterization of FLG. (a) The calculated graphene layer number distribution (color bar) based on optical transmittance image (Figure S1a). (b) SEM image of FLG.

consists of graphene islands ranging from 15 to 18 layers and a base of $\sim\!\!3$ layers of graphene. The SEM image (Figure 1b) reveals a $1.7\pm0.9~\mu\mathrm{m}^2$ grain size of FLG crystals. This height distribution was confirmed by mapping of the G peak (1585 cm $^{-1}$) of the FLG Raman spectra (Figure S1b). Increased layer number lead to increased G peak intensity (Figure S1c and Table S1). The micron-sized dimension and the distribution of thick FLG islands ensures fast alkali ion transport within each domain. 25

We evaluated K⁺ intercalation into FLG via cyclic voltammetry (CV) in 0.1 M KPF₆ in PC-EC (1:1 vol./vol.) solution to analyze the peaks corresponding to the progressive filling of graphene interlayers, i.e. ion-staging, ^{20,26,27} and the identification of metal plating. Reported potentials are referenced to 0.1 M Li⁺/Li hereafter. When sweeping the potential of FLG negative in K⁺ containing electrolyte at 1 mVs⁻¹ (Figure 2a trace-1), no K⁺ intercalation peaks were found. Instead, an irreversible reductive deposition process was observed (0.7 to 0.2 V) as indicated by the crossing of forward and backward traces.⁵ In contrast, when the solution was replaced with 0.1 M LiBF₄ in PC-EC, the FLG displayed clear staging-type Li⁺ intercalation behavior (Figure 2a trace-2).²⁶

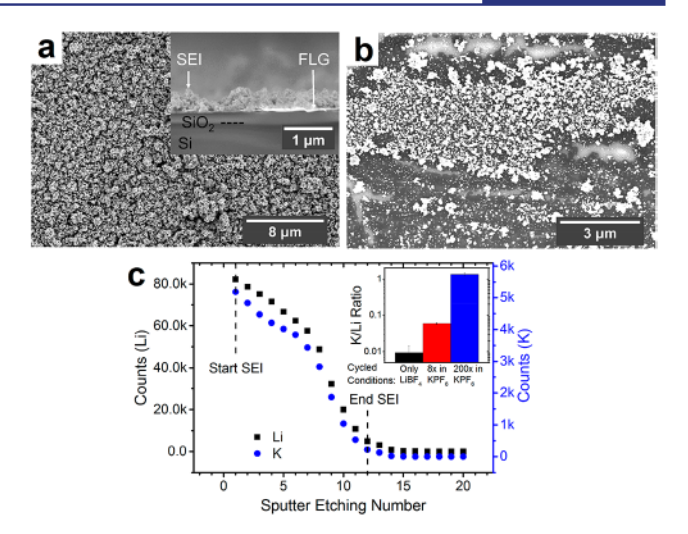


Figure 3. Postexperimental SEM and TOF-SIMS analysis. (a) SEM image of FLG with stable K^{+} intercalation performance. Inset: cross sectional image of same sample. (b) SEM image of FLG which exhibit K plating. (c) TOF-SIMS depth profiling results of FLG with full Li⁺ based SEI conditioning and exposure to few cycles in K^{+} containing electrolyte. Inset: K/Li counts ratio for FLG samples under different conditions.

Direct K⁺ intercalation is not readily accessible in pristine FLG at the rates and conditions under which Li⁺ intercalation occurs. Since Li⁺ intercalation creates structural changes on graphitic anode, ²⁸ we expected that testing the previous electrode in K⁺ containing electrolyte would exhibit also K⁺ intercalation. However, further polarizing the FLG in 0.1 M KPF₆ (Figure 2b trace-3) yielded only K plating and stripping. After this, Li⁺ no longer intercalated into FLG (Figure S2b), with the electrode displaying Li plating and stripping as well (Figure 2b trace-4). Therefore, an SEI inherently formed in K⁺

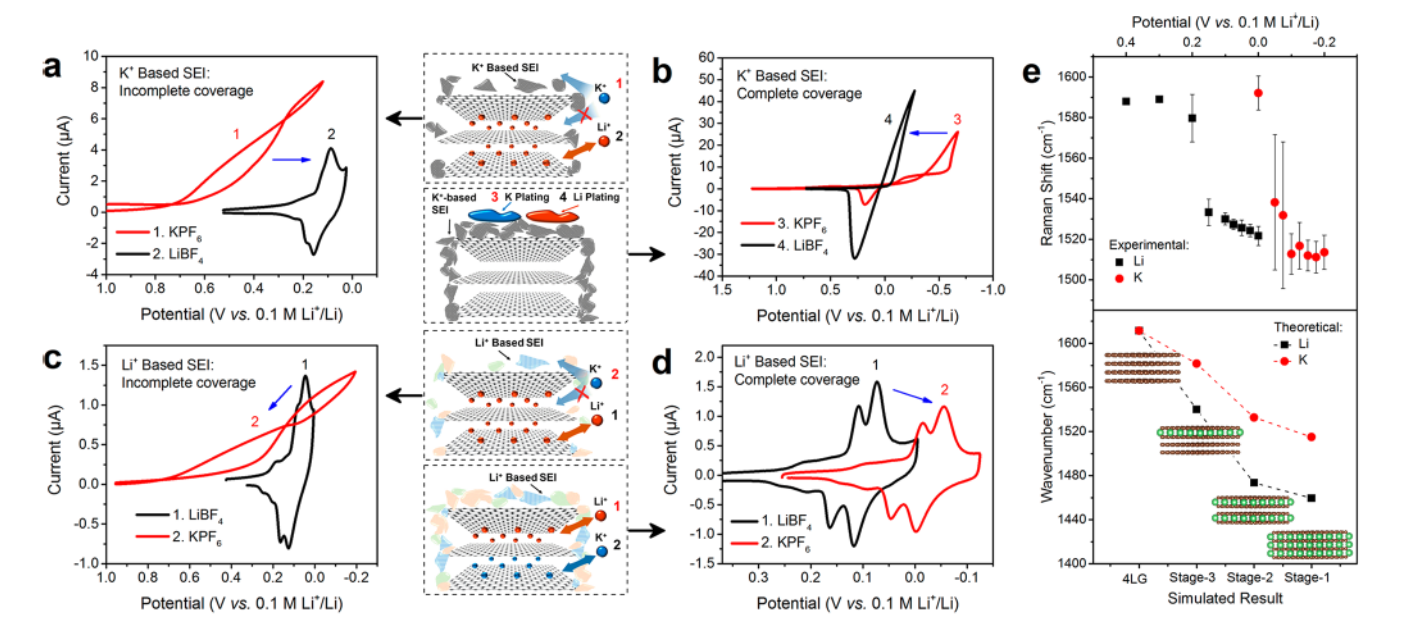


Figure 2. Effect of SEI conditioning in Li⁺ and K⁺ electrolytes. Panels a and b: sequential tests of pristine FLG with SEI initially formed in K⁺ containing solution at different degree of coverage. Panels c and d: same as panels a and b, but with SEI formed in Li⁺ containing solution. Number labels on CV traces correspond to chronological order of experimental procedure. (e) Raman G peak position change during Li⁺ or K⁺ intercalation and its comparison with theoretical *ab initio* calculations. All experiments were tested in 0.1 M LiBF₄ or 0.1 M KPF₆ in PC-EC, on 4.9 mm² FLG working electrode at 1 mV s⁻¹.

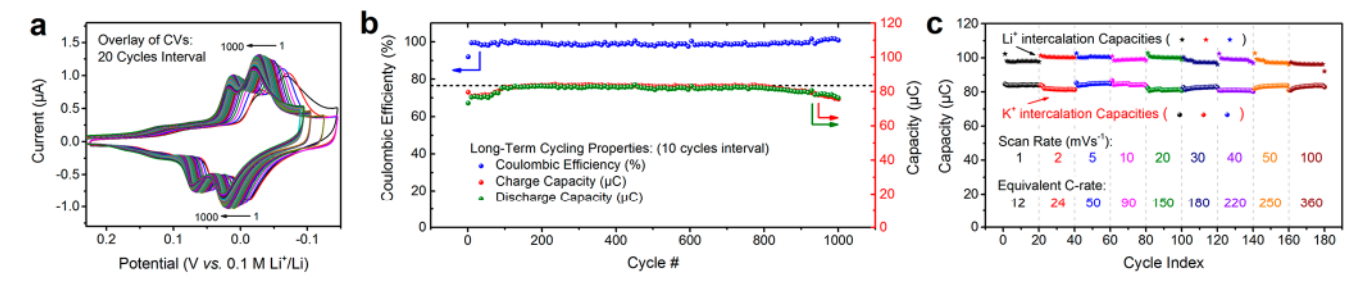


Figure 4. Long-term cycling and fast scan properties. (a) Long-term cycling study of K⁺ intercalation on FLG for 1000 cycles at 1 mV s⁻¹. (b) Charge-discharge capacities under all (de)intercalation peaks and Coulombic efficiencies. The theoretical capacity is indicated by the dashed line. (c) Li⁺ and K⁺ charge capacities at various scan rates up to 100 mV s⁻¹. Each scan rate condition was tested for 20 cycles. All experiments were tested in 0.1 M LiBF₄ or 0.1 M KPF₆ in PC-EC, on 4.9 mm² FLG working electrode at 1 mV s⁻¹ (panel a) or varies scan rates listed in figure legend (panel c).

containing electrolyte does not favor reversible intercalation

Given our observation and recent reports that SEIs formed in K+ containing electrolytes lead to deficient intercalation properties, 7,19 we hypothesized that a preformed Li⁺ based SEI layer would benefit K+ intercalation. To accomplish this, the FLGs were preconditioned in LiBF4 solution to form a fully passivated SEI layer (Figure S3). Following this pretreatment, K⁺ intercalation peaks were now well-defined (Figure 2d). The similarities between Li+ and K+ intercalation signatures on preconditioned FLG suggests a comparable staging-type intercalation process. Comparing the Li+ and K+ signals, four groups of (de)intercalation peaks were identified (Table S2), which we attribute to phase transitions between the different intercalation stages. 5,29 Galvanostatic charge—discharge at 10C (equivalent to 1 mV s⁻¹ scan rate in CV) revealed similar ion storage properties for both Li⁺ and K⁺ (Figure S4). We define 1C-rate as the full use of the FLG capacity during lithiation or potassiation in 1 h. Integrating the charge in Figure 2d, we found a Li+/K+ ratio of 1.33 and 1.32 for intercalation and deintercalation peaks, respectively (Table S2). This trend agrees with the stoichiometric changes between LiC6 and KC_{8}^{30} which yields a theoretical ratio of 1.33. To confirm that Li+ and K+ were involved in distinct intercalation processes, in situ Raman measurements were obtained during each ion insertion (Figure 2e-top). Ab initio calculations were also used to compute Raman active frequencies at different intercalation stages of Li⁺ or K⁺ on a four-layer graphene (4LG) model system (Figure 2e-bottom). Both methods agree well; a gradual displacement of the G peak was observed upon intercalation. The observable red shift can be explained by the intercalated ions inducing strain in the graphene.³¹

We attribute the reversible K⁺ intercalation behavior to the preconditioned Li+ based SEI layer on the FLG. As a comparison, insufficient conditioning with fewer cycles leads to incomplete coverage of the SEI and subsequent inhibition of K⁺ intercalation (Figure 2c). These experiments support the crucial role of the Li+ based SEI coverage for K+ intercalation and highlight the importance of forming a suitable layer from the beginning. The choice of the reference electrode does not affect the electrode behavior (Figure S5). Furthermore, the lack of noticeable intercalation response when using the bulky tetrabutylammonium cation (Figure S6) validates that the origin of observed staging-type peaks come from K+ uptake and not from the remaining Li+ in the preformed SEI.

To further elucidate the role of the SEI layer on enabling facile K+ intercalation, we performed postexperimental SEM

and TOF-SIMS analysis. The entire surface of preconditioned FLG capable of intercalating K⁺ is covered by submicron sized SEI clusters (Figure 3a) with more than 200 nm thickness (Figure 3a inset), comparable to the binder free graphite SEI morphology.³² In contrast, FLG displaying a patchy surface as a result of insufficient SEI conditioning (Figure 3b) was prone to metal plating and instabilities at large negative electrode polarization (Figure 2c). In TOF-SIMS depth profiling, the coexistence of elemental Li and K was verified in preconditioned FLG that had undergone few K+ intercalation cycles (Figure 3c). The presence of both alkali ions decreases at a similar fashion as the SEI was removed. An FLG sample cycled exclusively in LiBF4 showed near to zero K/Li ratio throughout. In contrast, FLG cycled 200 times in KPF6 led to a dramatic increase of atomic K, marked by a 23-fold rise in the K/Li ratio (Figure 3c inset). These observations support the idea that K⁺ diffused through the preformed Li⁺ based SEI. We hypothesize that the progressive substitution of Li+ with K+ in the SEI results in a favorable interface for K+ transport and provides a framework that supports reversible electrochemical intercalation of K+.

A preconditioned SEI layer also promotes long-term K⁺ intercalation with a fully reversible behavior at the fast chargedischarge rate of 10C for at least 1000 cycles (Figure 4). Continuous K+ transport through the SEI likely leads to a gradual cationic substitution between Li+ and K+ during the first ~100 cycles, resulting in a lower overpotential to intercalate K+ (Figure 4a, Figure S7). We postulate the decrease in (dis)charge capacities around the 800th cycle arises from changes in the electrolyte composition and accessible FLG area on the open electrochemical cell used in this study over the 8 days of testing. The theoretical capacity of K+ uptake was estimated at 83.5 µC based on Li⁺ capacity (Figure S8). The majority of the charge-discharge cycles display capacities around the theoretical limit (Figure 4b). The capacity was also retained at 90.6% toward the 1000th cycle, with a Coulombic efficiency of 99.2 ± 0.8% throughout all cycles (Figure 4b). The CV features observed at 1 mV s⁻¹ for the long-term cycling experiments compare positively against the best reported K+ intercalation CVs, performed at a scan rate 100 times slower than our work. Full capacity retention with discernible staging profile were further maintained at even faster scan rates up to 100 mV s⁻¹ for both Li⁺ and K⁺ (Figure 4c and Figure S9), equivalent to charge-discharge C-rates of 360. Galvanostatic charge-discharge results revealed similar fast cycling behavior (Figure S10). To the best of our

knowledge, this is the fastest charge-discharge reported for K+ intercalation on a graphitic material.

In summary, we explored the role of SEI preconditioning on FLG electrodes for K+ intercalation. Conditioning the FLG with a Li+ based SEI with full electrode coverage enabled well resolved staging-type K+ intercalation. This simple strategy enables the intercalation of K⁺ on graphitic materials at least 2 orders of magnitude faster than any published work, and with a near theoretical K+ storage. The preformed SEI layer further protects the FLG electrode for at least 1000 CV cycles, with distinctly observable intercalation stages and high capacity retention. Ion intercalation was confirmed via in situ Raman spectroscopy, while the K+ penetration through the SEI and Li/K ion exchange during cycling was confirmed by TOF-SIMS analysis. This work highlights the functionality of the SEI on controlling alkali ion intercalation mechanisms and the versatility of large-area FLG electrodes for exploring fundamental aspects of intercalation chemistry. We speculate that the SEI plays a prominent role in the electrochemical intercalation signatures and stability of a wide variety of mono or multivalent ions into carbon based anodes. This work shows a simple and attractive pathway toward electrode design for high-performance beyond Li-ion technologies.

ASSOCIATED CONTENT

Supporting Information

The Supporting Information is available free of charge on the ACS Publications website at DOI: 10.1021/jacs.8b08907.

Details of chemicals; graphene growth; Raman characterization of FLG; SEI formation conditions; control experiments using various cations and reference electrodes; K+ long-term cycling properties; galvanostatic analysis; TOF-SIMS results; reference calibration; DFT simulation details (PDF)

AUTHOR INFORMATION

Corresponding Authors

*mendoza@eng.famu.fsu.edu

*joaquinr@illinois.edu

ORCID ®

Jingshu Hui: 0000-0002-6987-4414 Noah B. Schorr: 0000-0002-1582-8594 Srimanta Pakhira: 0000-0002-2488-300X Jose L. Mendoza-Cortes: 0000-0001-5184-1406 Joaquín Rodríguez-López: 0000-0003-4346-4668

Author Contributions

[¶]J.H., N.B.S., and S.P. contributed equally.

Notes

The authors declare no competing financial interest.

ACKNOWLEDGMENTS

This material is based upon work supported by the National Science Foundation under Grant No. NSF DMR 16-11268. Sample preparation and characterization were carried out in part in the Frederick Seitz Materials Research Laboratory Central Facilities, University of Illinois. We thank Prof. Andrew Gewirth's group for providing a Li electrode for the in situ Raman cell, and Mr. Dipobrato Sarbapalli for help in writing Matlab code for data analysis. S.P. also thanks the SERB-DST, Govt. of India for providing the Ramanujan Faculty Fellowship. S.P. and J.L.M-C. thank the High-Performance Computer (HPC) at the Research Computing Center in Florida State University (FSU) for providing computational resources and support.

REFERENCES

- (1) Taylor, S. R. Abundance of Chemical Elements in the Continental Crust - a New Table. Geochim. Cosmochim. Acta 1964, 28, 1273-1285.
- (2) Nossol, E.; Souza, V. H. R.; Zarbin, A. J. G. Carbon Nanotube/ Prussian Blue Thin Films as Cathodes for Flexible, Transparent and ITO-Free Potassium Secondary Battery. J. Colloid Interface Sci. 2016,
- (3) Wessells, C. D.; Peddada, S. V.; Huggins, R. A.; Cui, Y. Nickel Hexacyanoferrate Nanoparticle Electrodes for Aqueous Sodium and Potassium Ion Batteries. Nano Lett. 2011, 11, 5421-5425.
- (4) Matsuura, N.; Umemoto, K.; Takeuchi, Z. Standard Potentials of Alkali-Metals, Silver, and Thallium Metal-Ion Couples in N,N'-Dimethylformamide, Dimethyl-Sulfoxide, and Propylene Carbonate. Bull. Chem. Soc. Jpn. 1974, 47, 813-817.
- (5) Komaba, S.; Hasegawa, T.; Dahbi, M.; Kubota, K. Potassium Intercalation into Graphite to Realize High-Voltage/High-Power Potassium-Ion Batteries and Potassium-Ion Capacitors. Electrochem. Commun. 2015, 60, 172-175.
- (6) Luo, W.; Wan, J. Y.; Ozdemir, B.; Bao, W. Z.; Chen, Y. N.; Dai, J. Q.; Lin, H.; Xu, Y.; Gu, F.; Barone, V.; Hu, L. B. Potassium Ion Batteries with Graphitic Materials. Nano Lett. 2015, 15, 7671-7677.
- (7) Xing, Z. Y.; Qi, Y. T.; Jian, Z. L.; Ji, X. L. Polynanocrystalline Graphite: A New Carbon Anode with Superior Cycling Performance for K-Ion Batteries. ACS Appl. Mater. Interfaces 2017, 9, 4343-4351.
- (8) Jian, Z. L.; Luo, W.; Ji, X. L. Carbon Electrodes for K-Ion Batteries. J. Am. Chem. Soc. 2015, 137, 11566-11569.
- (9) Zhao, J.; Zou, X. X.; Zhu, Y. J.; Xu, Y. H.; Wang, C. S. Electrochemical Intercalation of Potassium into Graphite. Adv. Funct. Mater. 2016, 26, 8103-8110.
- (10) Vaalma, C.; Giffin, G. A.; Buchholz, D.; Passerini, S. Non-Aqueous K-Ion Battery Based on Layered K03MNO2 and Hard Carbon/Carbon Black. J. Electrochem. Soc. 2016, 163, A1295-A1299.
- (11) Jian, Z. L.; Xing, Z. Y.; Bommier, C.; Li, Z. F.; Ji, X. L. Hard Carbon Microspheres: Potassium-Ion Anode Versus Sodium-Ion Anode. Adv. Energy Mater. 2016, 6, 1501874.
- (12) Barton, Z. J.; Hui, J.; Schorr, N. B.; Rodríguez-López, J. Detecting Potassium Ion Gradients at a Model Graphitic Interface. Electrochim. Acta 2017, 241, 98-105.
- (13) Share, K.; Cohn, A. P.; Carter, R.; Rogers, B.; Pint, C. L. Role of Nitrogen-Doped Graphene for Improved High-Capacity Potassium Ion Battery Anodes. ACS Nano 2016, 10, 9738-9744.
- (14) Ju, Z. C.; Zhang, S.; Xing, Z.; Zhuang, Q. C.; Qiang, Y. H.; Qian, Y. T. Direct Synthesis of Few-Layer F-Doped Graphene Foam and Its Lithium/Potassium Storage Properties. ACS Appl. Mater. Interfaces 2016, 8, 20682-20690.
- (15) Share, K.; Cohn, A. P.; Carter, R. E.; Pint, C. L. Mechanism of Potassium Ion Intercalation Staging in Few Layered Graphene from in Situ Raman Spectroscopy. Nanoscale 2016, 8, 16435-16439.
- (16) Agubra, V. A.; Fergus, J. W. The Formation and Stability of the Solid Electrolyte Interface on the Graphite Anode. J. Power Sources 2014, 268, 153-162.
- (17) Kong, F.; Kostecki, R.; Nadeau, G.; Song, X.; Zaghib, K.; Kinoshita, K.; McLarnon, F. In Situ Studies of SEI Formation. J. Power Sources 2001, 97-98, 58-66.
- (18) Verma, P.; Maire, P.; Novák, P. A Review of the Features and Analyses of the Solid Electrolyte Interphase in Li-Ion Batteries. Electrochim. Acta 2010, 55, 6332-6341.
- (19) Chandrasiri, K. W. D. K.; Nguyen, C. C.; Zhang, Y. Z.; Parimalam, B. S.; Lucht, B. L. Systematic Investigation of Alkali Metal Ions as Additives for Graphite Anode in Propylene Carbonate Based Electrolytes. Electrochim. Acta 2017, 250, 285-291.
- (20) Hui, J.; Burgess, M.; Zhang, J.; Rodríguez-López, J. Layer Number Dependence of Li⁺ Intercalation on Few-Layer Graphene

- and Electrochemical Imaging of Its Solid-Electrolyte Interphase Evolution. ACS Nano 2016, 10, 4248-4257.
- (21) Cristarella, T. C.; Chinderle, A. J.; Hui, J.; Rodríguez-López, J. Single-Layer Graphene as a Stable and Transparent Electrode for Nonaqueous Radical Annihilation Electrogenerated Chemiluminescence. *Langmuir* 2015, 31, 3999–4007.
- (22) Hui, J.; Pakhira, S.; Bhargava, R.; Barton, Z. J.; Zhou, X.; Chinderle, A. J.; Mendoza-Cortes, J. L.; Rodríguez-López, J. Modulating Electrocatalysis on Graphene Heterostructures: Physically Impermeable yet Electronically Transparent Electrodes. ACS Nano 2018, 12, 2980–2990.
- (23) Hui, J.; Zhou, X.; Bhargava, R.; Chinderle, A.; Zhang, J.; Rodríguez-López, J. Kinetic Modulation of Outer-Sphere Electron Transfer Reactions on Graphene Electrode with a Sub-Surface Metal Substrate. *Electrochim. Acta* 2016, 211, 1016–1023.
- (24) Graf, D.; Molitor, F.; Ensslin, K.; Stampfer, C.; Jungen, A.; Hierold, C.; Wirtz, L. Spatially Resolved Raman Spectroscopy of Single- and Few-Layer Graphene. *Nano Lett.* 2007, 7, 238–242.
- (25) Levi, M. D.; Aurbach, D. Diffusion Coefficients of Lithium Ions During Intercalation into Graphite Derived from the Simultaneous Measurements and Modeling of Electrochemical Impedance and Potentiostatic Intermittent Titration Characteristics of Thin Graphite Electrodes. J. Phys. Chem. B 1997, 101, 4641–4647.
- (26) Levi, M. D.; Aurbach, D. Simultaneous Measurements and Modeling of the Electrochemical Impedance and the Cyclic Voltammetric Characteristics of Graphite Electrodes Doped with Lithium. *J. Phys. Chem. B* 1997, 101, 4630–4640.
- (27) Lopez, J. L. L.; Grandinetti, P. J.; Co, A. C. Enhancing the Real-Time Detection of Phase Changes in Lithium-Graphite Intercalated Compounds through Derivative Operando (dOp) NMR Cyclic Voltammetry. J. Mater. Chem. A 2018, 6, 231–243.
- (28) Dahn, J. R. Phase-Diagram of Li_xC₆. Phys. Rev. B: Condens. Matter Mater. Phys. 1991, 44, 9170-9177.
- (29) Eftekhari, A.; Jian, Z. L.; Ji, X. L. Potassium Secondary Batteries. ACS Appl. Mater. Interfaces 2017, 9, 4404-4419.
- (30) Wang, Z. H.; Selbach, S. M.; Grande, T. Van der Waals Density Functional Study of the Energetics of Alkali Metal Intercalation in Graphite. RSC Adv. 2014, 4, 4069–4079.
- (31) Zou, J.; Sole, C.; Drewett, N. E.; Velický, M.; Hardwick, L. J. *In Situ* Study of Li Intercalation into Highly Crystalline Graphitic Flakes of Varying Thicknesses. *J. Phys. Chem. Lett.* 2016, 7, 4291–4296.
- (32) Nie, M. Y.; Chalasani, D.; Abraham, D. P.; Chen, Y. J.; Bose, A.; Lucht, B. L. Lithium Ion Battery Graphite Solid Electrolyte Interphase Revealed by Microscopy and Spectroscopy. J. Phys. Chem. C 2013, 117, 1257—1267.